Characterization of Electrospun PVdF Fiber-Based Polymer Electrolytes

Sung Won Choi,[†] Jeong Rae Kim,[‡] Young Rack Ahn,[§] Seong Mu Jo,*[,§] and Elton J. Cairns[⊥]

Materials Science and Engineering Program, University of Texas at Austin, Austin, Texas 78712, and SKC Co., Ltd., #460 Chonhung-ri, Songgo-ub, Chonan-city, Chungchongnam-do 330-836, Korea, Optoelectronic Materials Research Center, Korea Institute of Science and Technology, 39-1 Hawolgok-dong, Seongbuk-gu, Seoul 136-791, Korea, and Advanced Energy Technologies Department, Lawrence Berkeley National Laboratory, 1 Cyclotron Road, Berkeley, California 94720-8168

Received January 27, 2006. Revised Manuscript Received July 16, 2006

Porous PVdF fiber-based membranes with a three-dimensional network structure, high porosity, large electrolyte solution uptake, and adequate mechanical properties were prepared by an electrospinning technique using various mixed-solvent compositions with poly(vinylidene fluoride) (PVdF). Their physical properties, including surface morphology, average fiber diameter, pore size, and electrolyte solution uptake, strongly depended on the composition of the polymer solution used for electrospinning. From X-ray diffraction and FT-Raman data, we found the PVdF membranes to have mixed-crystal structure sof Form II (α-type) and Form III (γ-type). Electrospun PVdF fiber-based polymer electrolytes were prepared by immersing porous PVdF membranes into 1 M $LiPF_6$ electrolyte solutions. On the basis of FT-Raman data of the PVdF fiber-based polymer electrolytes, it was shown that ethylene carbonate molecules mainly participated in the solvation of the lithium salt. Moreover, with the exception of diethyl carbonate, these aliphatic carbonate molecules strongly interacted with the PVdF chain. The polymer electrolytes exhibited high ionic conductivities up to 1.0×10^{-3} S/cm at room temperature, and wide electrochemical stability windows of 0.0 to 4.5 V vs Li/Li^+. The ionic conductivity of the PVdF fiber-based polymer electrolytes depended on the physicochemical properties of the 1 M $LiPF_6$ electrolyte solution inside the pores, whereas their electrochemical properties were enhanced by the interaction between the PVdF chain and the aliphatic carbonate molecules. Thus, prototype cells with PVdF fiber-based polymer electrolytes showed a range of different charge/discharge properties according to the solvent composition of the 1 M $LiPF_6$ electrolyte solutions and the C-rate. In addition, the cycling performances depended on the electrochemical and spectroscopic properties of the electrospun PVdF fiber-based polymer electrolytes.

1. Introduction

Electrospinning has been widely used as a simple yet powerful technique to produce ultrathin fibers and their corresponding membranes.[1−3] In the electrospinning of polymer solutions, a number of parameters are known to affect the physical properties of the electrospun fibers, including fiber shape, diameter, surface morphology, and porosity.[4−6] These governing parameters can be classified into three major categories: (1) internal parameters, including the nature and molecular weight of the polymer and the physical properties of the polymer solution (concentration, viscosity, conductivity, dielectric permeability, and surface tension); (2) process parameters, including the applied potential, the hydrostatic pressure in the capillary tube, the distance between the tip and the collector, the feed rate, and the size of the nozzle; and (3) ambient parameters, including temperature, humidity, and air flow in the electrospinning chamber. Current research is mainly focused on controlling these internal parameters, as these represent the most important factors for determining the physical properties of the electrospun fibers and their membranes.[7,8] On the other hand, electrospun fibers and their corresponding membranes also have their own unique properties, such as average fiber diameters in the submicrometer range, high porosities, large surface areas, fully interconnected pore structures, and sufficient mechanical strengths. These outstanding properties make electrospun fibers attractive for a wide range of applications, including tissue engineering, wound dressing, military protective clothing, filter media, as well as nanosensor and electronics applications.[9−11]

* Corresponding author. Telephone: 82-2-958-5355. Fax: 82-2-958-5309. E-mail: smjo@kist.re.kr.
[†] University of Texas at Austin.
[‡] SKC Co., Ltd.
[§] Korea Institute of Science and Technology.
[⊥] Lawrence Berkeley National Laboratory.

(1) Wang, X.; Drew, C.; Lee, S. H.; Senecal, K. J.; Kumer, J.; Samuelson, L. A. *Nano Lett.* **2002**, *2*, 1273.
(2) Tsai, P. P.; Gibson, H. S.; Gibson, P. *J Electrostat.* **2002**, *54*, 333.
(3) Reneker, D. H.; Yarin, A. L.; Fong, H.; Koombhongse, S. J. *J. Appl. Phys.* **2000**, *87*, 4531.
(4) Casper, C. L.; Stephenes, J. S.; Tassi, N. G.; Bruce, Chase, D.; Rablot, J. F. *Macromolecules* **2004**, *37*, 573.
(5) Theron, S. A.; Zussman, E.; Yarin, A. L. *Polymer* **2004**, *45*, 2017.
(6) Mit-uppatham, C.; Nithitanakul, M.; Supaphol, P. *Macromol. Chem. Phys.* **2004**, *205*, 2327.
(7) Lee, J. S.; Choi. K. H,; Ghim, H. D.; Kim, S. S.; Chun, D. H.; Kim, H. Y.; Lyoo, W. S. *J. Appl. Polym. Sci.* **2004**, *93*, 1638.
(8) Wannatong, L.; Sirivat, A.; Supaphol, P. *Polym. Int.* **2004**, *53*, 1851.
(9) Subbiah, T.; Bhat, G. S.; Tock, R. W.; Parameswaran, S.; Ramkumar, S. S. *J. Appl. Polym. Sci.* **2005**, *96*, 557.

10.1021/cm060223+ CCC: $37.00
Published on Web 12/05/2006

In recent years, we have shown that electrospun membranes can also be used as polymer electrolytes in lithium cells.[12−13] It is suggested that electrospun PVdF nanofiber-based membranes will make good polymer matrices for use as separators, on account of their high porosity, high surface area, and fully interconnected open pore structures. These electrospun PVdF nanofiber-based membranes also have attractive electrochemical properties, including high ionic conductivity, wide electrochemical stability windows, and moderate interfacial resistance toward lithium metal electrodes. In a further study, we investigated the interaction between the PVdF polymer chain and the molecules of the electrolyte solution and monitored their effects on the electrochemical properties of electrospun PAN fiber-based polymer electrolytes and their prototype cells.[14] From this study, we suggested that the ethylene carbonate (EC) molecules of the polymer chain mainly interacted with the lithium ions in the electrolyte, where the solvated lithium ions resulted in good ionic conduction. On the other hand, aliphatic carbonate molecules, such as dimethyl carbonate (DMC), ethylmethyl carbonate (EMC), and diethyl carbonate (DEC), were found to associate with the nitrile groups of the PAN chain, participating in the swelling of the PAN fibers. The electrochemical properties of PAN fiber-based polymer electrolytes were significantly enhanced by the swelling of the electrospun PAN fibers. Although the PAN fiber-based framework was observed to swell in electrolyte solution, the network was maintained during electrochemical cycling and showed adequate mechanical properties.

In the present study, we investigated the physical and mechanical properties of electrospun PVdF fiber-based membranes prepared from polymer solutions comprising various compositions of mixed-solvent systems. We also investigated the electrochemical properties of the electrospun PVdF fiber-based polymer electrolytes for application in lithium-ion polymer batteries. The interactions between the PVdF fibers, lithium ions, and solvent molecules were characterized using vibrational spectroscopic techniques to investigate their effect on the electrochemical properties of electrospun PVdF fiber-based polymer electrolytes. Prototype cells were then fabricated from these polymer electrolytes, and their cycling performances were investigated in various electrolyte solutions.

2. Experimental Section

2.1. Preparation of Samples. Polymer solutions for electrospinning were prepared from 17 wt % poly(vinylidene fluoride) (PVdF, Atofina, Kynar 761, $M_w = 5.2 \times 10^5$) and several mixed-solvent systems, as shown in Table 1. Before preparing the polymer solutions, the PVdF material was dried under a vacuum at 80 °C for 12 h to eliminate moisture and volatile impurities. HPLC-grade solvents (Merck) were used in the electrospinning experiments without further treatment. The polymer and mixed solvents were stirred at 80 °C to form a transparent and homogeneous polymer solution, which was then cooled to room temperature. The viscosities of the PVdF polymer solutions (200 mL) were determined using a DV−II+ viscometer (Brookfield), where the temperature was maintained at 30 °C using an oil bath, hotplate (IKA, RCT basic IKAMAG), and thermocouple (IKA, IKA ETS-D 4 Fuzzy IKATRON). The rotating speeds of the S2 and S3 spindles ranged between 20 and 100 rpm.

Table 1. Solvent Compositions of the Polymer Solutions Used for Electrospinning

	solvent composition (wt %)	
sample	acetone	DMAc[a]
ESM-1	100	
ESM-2	90	10
ESM-3	80	20
ESM-4	70	30
ESM-5	60	40
ESM-6	50	50

[a] *N*,*N*-Dimethylacetamide.

Porous PVdF membranes were prepared using a typical electrospinning method with a vertical arrangement.[1−2] A stainless steel needle (24 G, outer diameter: 0.58 mm, inner diameter: 0.30 mm) was connected to a high-voltage power supply (Bertan, model 230), and polymer solution was then supplied to the needle using a syringe infusion/withdrawal pump (KD scientific, model 220). A high voltage of 15 kV was then applied to the end of the needle. The electrospun PVdF membranes were then deposited on to grounded, polished stainless steel plates, where the tip−ground distance was fixed at 12 cm. Each membrane (thickness 30 μm) was dried in a vacuum oven at 80 °C to remove any remaining solvent and then stored in a glove box filled with Ar gas (H_2O <1 ppm) prior to use.

PVdF fiber-based polymer electrolytes were prepared by soaking the electrospun PVdF membranes in electrolyte solutions of either 1 M $LiPF_6$−EC/DMC (2/1, wt/wt), 1 M $LiPF_6$−EC/DMC (1/1, wt/wt), 1 M $LiPF_6$−EC/EMC (1/1, wt/wt), 1 M $LiPF_6$−EC/DEC (1/1, wt/wt), or 1 M $LiPF_6$−EC/DMC/DEC (1/1/1, wt/wt/wt) (Merck, battery grade) at room temperature. All processes were carried out under an argon atmosphere (H_2O <1 ppm).

Prototype cells were assembled by sandwiching polymer electrolytes between a mesocarbon microbead (MCMB) anode (SKC supplied, Korea) and $LiCoO_2$ cathode (SKC supplied, Korea) under an argon atmosphere (H_2O <1 ppm). These cells were then vacuum-sealed in an aluminum-plastic pouch and stored at 50 °C prior to performing the cycling tests. The theoretical capacity of the $LiCoO_2$ cathode was determined to be about 145 mAh/g at a cycling rate of C/5.

2.2. Characterization of Samples. *Physical and Chemical Properties of Electrospun PVdF membranes and Its Polymer Electrolytes.* The morphology of the electrospun PVdF membranes was observed using field-enhanced scanning electron microscopy (FE-SEM, Hitachi, S-4200) under vacuum conditions. All samples were gold-coated prior to SEM measurements. The average fiber diameter of each sample was calculated using appropriate software (SigmaScanPro 5.0, SPSS) and on the basis of SEM images of magnification ×5000.

The mean pore diameters were measured using a capillary flow porometer (PMI, ver. 7.0) within a pressure range of 0−30 psi. The pore size was calculated from the resulting wet and dry flow curves. Perfluoropolyether (propene 1,1,2,3,3,3 hexafluoro, oxidized, polymerized) was used as a wetting agent.

To investigate the electrolyte solution uptake, we cut the electrospun PVdF membranes into 3 × 3 cm samples and then

(10) Li, D.; Xia, Y. *Adv. Mater.* **2004**, *16*, 1151.
(11) Huang, Z.-M.; Zhang, Y.-Z.; Kotaki, M.; Ramakrishna, S. *Compos. Sci. Technol.* **2003**, *63*, 2223.
(12) Kim, J. R.; Choi, S. W.; Jo, S. M.; Lee, W. S.; Kim, B. C. *Electrochim. Acta* **2004**, *50*, 69.
(13) Choi, S. W.; Jo, S. M.; Lee, W. S.; Kim, Y.-R. *Adv. Mater.* **2003**, *15*, 2027.
(14) Choi, S. W.; Kim, J. R.; Jo, S. M.; Lee, W. S.; Kim, Y. R. *J. Electrochem. Soc.* **2005**, *152*, A989.

soaked them in 1 M $LiPF_6$−EC/DMC/DEC (1/1/1, wt/wt/wt). The excess electrolyte solution remaining on the membrane surface was removed by wiping it with filter paper.

The electrospun PVdF membrane samples were exposed to the same conditions as those in the electrochemical cells. The weight of the electrospun PVdF membranes soaked with electrolyte solution was measured as a function of soaking time, and the amount of electrolyte solution uptake was calculated as the difference between the weights of the electrospun PVdF membranes, before and after electrolyte solution uptake.

The mechanical properties of the electrospun PVdF membrane samples (6.0 cm × 0.5 cm) were measured using a universal testing instrument (Instron, model 4464) at a cross-head speed of 10 mm/min and on the basis of the ASTM standard D882-95a at room temperature. Before testing, the thickness of the membrane was measured using a dial gauge (Mitsutoyo, BWB836).

Wide-angle X-ray diffraction (WAX) patterns of the electrospun PVdF membranes and their polymer electrolytes were obtained using an X-ray diffractometer (MAC Science, MX018) with CuKα radiation ($\lambda = 1.5405$). The samples were scanned in the range of 10−70° at room temperature. WAX experiments were performed at 40 kV and 100 mA, with a scan rate of 1°/min.

The vibrational spectra of the electrospun PVdF membranes and their polymer electrolytes were investigated using an FT-Raman spectrophotometer (Bruker, RFS-100/s) with a resolution of 1 cm^{-1}. The spectra were collected over the range of 400−3500 cm^{-1} by averaging 300. The individual peaks of the FT-Raman spectra were fitted with a trial function consisting of a baseline and Gaussian function (PeakFit 4.0, SPSS).

Electrochemical Properties of Ultrafine PVdF Fiber-Based Polymer Electrolytes. Ionic conductivity cells were assembled by sandwiching a given polymer electrolyte between two stainless steel blocking electrodes (2 cm × 2 cm) and were vacuum-sealed in an aluminum-plastic pouch in a dry box filled with argon gas. The ionic conductivity was determined over the frequency range of 0.1 Hz to 100 kHz at an AC amplitude of 10 mV and measured using the AC impedance technique (IM6e (Zahner Co.)) in the range from −20 to 60 °C.

The electrochemical stability windows of the PVdF fiber-based polymer electrolytes were determined using linear sweep voltammetry. These measurements were carried out using a three-electrode electrochemical cell consisting of a nickel working electrode and lithium reference and lithium counterelectrodes. An electrochemical analyzer (CHI, model 600) was utilized with a scan rate of 1 mV/s in the potential range of 0−5 V vs Li^+/Li.

The cycling of prototype cells with PVdF fiber-based polymer electrolytes was conducted with a battery cycler (WBCS3000, WonAtech Co.) at room temperature. The cell performance was evaluated galvanostatically with cutoff voltages of 2.75 and 4.2 V at different C-rates (0.5 and 1.0 C).

Before measuring the electrochemical properties, all cells were aged at 50 °C for 12 h and then cooled to room-temperature prior to taking measurements.

3. Results and Discussion

3.1. SEM Images of Electrospun PVdF Membranes. Figure 1 shows the SEM images of electrospun PVdF fiber-based membranes prepared from several mixed-solvent systems. The observed electrospun membranes consisted of fibers in the submicrometer range arranged in a three-dimensional network structure with high porosity and fully interconnected pores. Here, the average fiber diameter was found to decrease gradually with increasing concentration of DMAc in the mixed solvent. Thus, the surface morphology of the electrospun PVdF fibers largely depended on the mixed-solvent composition. With the exception of those electrospun PVdF fibers prepared using acetone and/or acetone/DMAc (9/1, wt/wt) as a solvent, most showed a smooth surface and cylindrical shape. When a high concentration of acetone was present in the polymer solution, the electrospun PVdF fiber showed a quite different morphology. The electrospun PVdF membrane prepared using acetone had irregular pores on the surface of the electrospun fibers, whereas that prepared in acetone/DMAC (9/1, wt/wt) contained some raised areas and wrinkles on the fiber surface. This morphological difference between the two fibers is due to the different behaviors of the solvent evaporation during electrospinning. Bognitzki et al. reported that fibers of partially crystalline poly-L-lactide (PLLA) produced using dichloromethane as a solvent had regular pore structures.[15] The formation of pore structures on the PLLA fibers is due to the rapid evaporation of the low-boiling-point dichloromethane solvent (about 40 °C) and high vapor pressure (475 mbar at 20 °C) during the fibers' flight to the collector. Bognitzki et al. suggested that a regular pore structure on the fibers was due to the regular phase morphology generated by rapid phase separation during the electrospinning process, such that the pore structures become oriented along the fiber axis. Thus, the solvent-rich regions are transformed into pores. When dichloromethane was replaced by a solvent with a high boiling point and low vapor pressure such as chloroform, pore formation was significantly reduced. In our case, using acetone as a solvent resulted in the formation of electrospun PVdF membranes whose fiber surfaces had irregularly oriented pores. This is because acetone has a higher boiling point and lower vapor pressure than dichloromethane. As a result of these solvent characteristics, the resulting pore sizes were quite irregular and nondirectional, and the pore size distribution was very broad. On the other hand, the electrospun PVdF membrane prepared from 17 wt % PVdF−acetone/DMAc (9/1, wt/wt) had fibers with several raised points and wrinkles along the fiber axis. It seems that DMAc has an influence on the process of solvent evaporation and solidification of the fiber during electrospinning. In this respect, the evaporation of acetone on the fiber surface will be hindered by the higher boiling point of DMAc, resulting in a surface morphology quite different from that obtained using acetone alone. However, further study is needed to explain such a unique morphology.

These results indicate that the surface morphology and fiber diameter of the electrospun PVdF membranes are significantly affected by the composition of the polymer solution used for electrospinning. The electrospun PVdF membranes formed in a mixed-solvent system with high acetone content have a unique surface morphology, including pores, wrinkles, and/or raised areas. Also, the fiber diameter was observed to decrease with increasing nonvolatile solvent (DMAc) content.

3.2. Physical Properties of Electrospun PVdF Membranes. The viscosity data in Figure 2 are shown as a function of the DMAc concentration in 17 wt % PVdF solutions for several mixed-solvent systems. Because DMAc

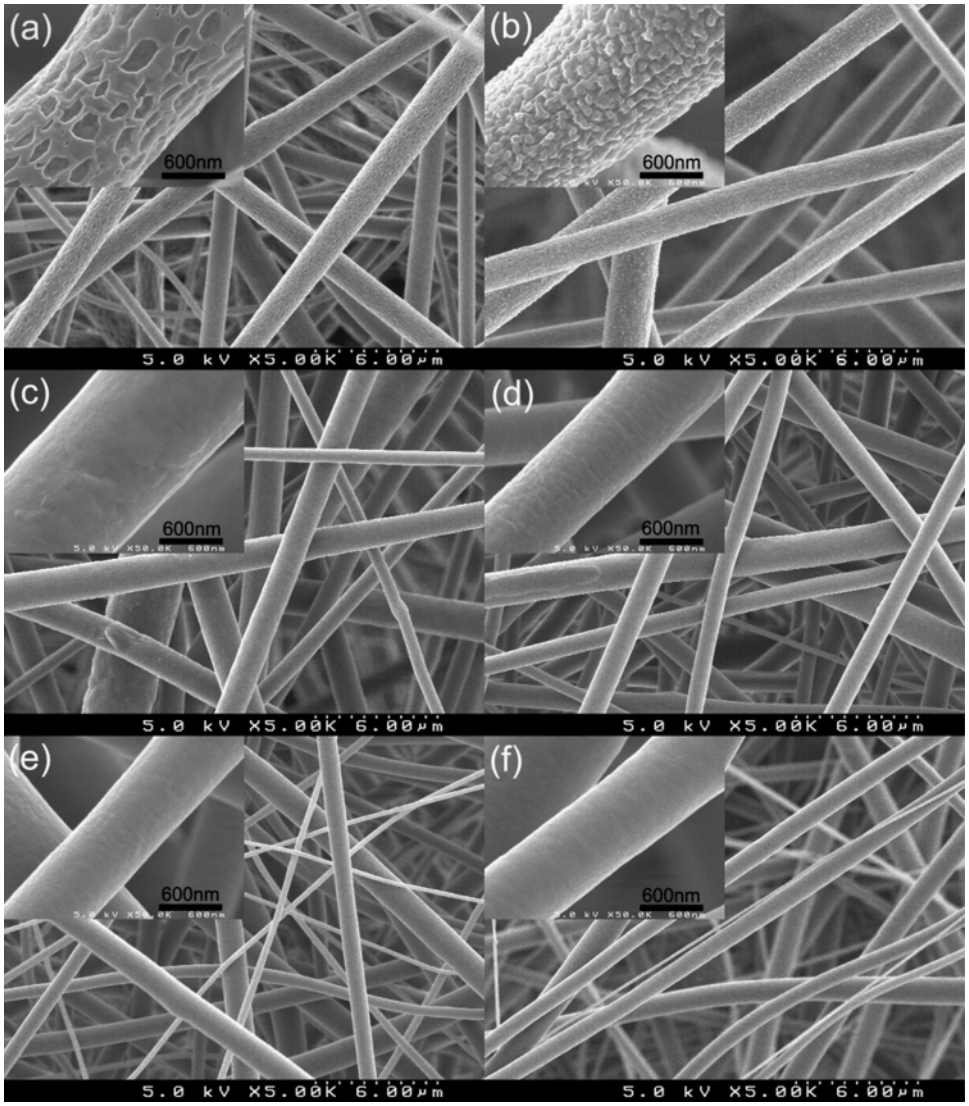

Figure 1. SEM images of the electrospun PVdF membranes prepared using (a) acetone, (b) acetone/DMAC (90/10), (c) acetone/DMAC (80/20), (d) acetone/DMAc (70/30), (e) acetone/DMAC (60/40), and (f) acetone/DMAc (50/50).

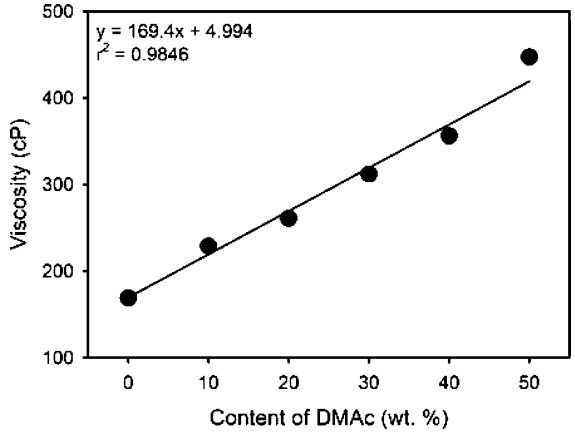

Figure 2. Viscosity data of the PVdF solutions as a function of DMAc concentration in 17 wt % PVdF solutions in various mixed-solvent systems.

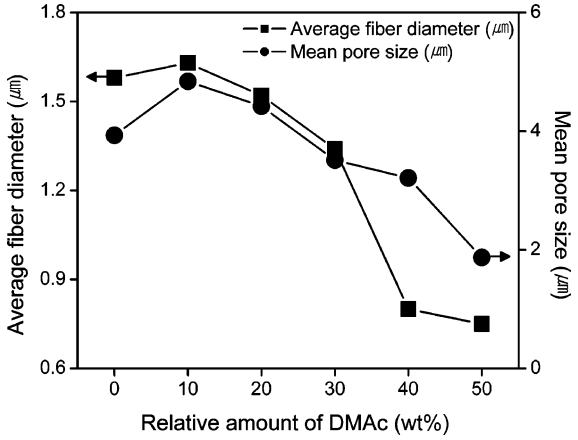

Figure 3. Average fiber diameter and mean pore size of the electrospun PVdF membranes as a function of the solvent composition in the polymer solution.

has a higher viscosity than acetone, the polymer solutions formed in a high content of DMAc had higher viscosities than those formed in solvents with a lower DMAc content. Thus, the viscosity of the polymer solution increased with increasing DMAc concentration in the mixed solvent, with the viscosity showing a good linear relationship with respect to the DMAc content in the mixed-solvent systems.

As shown in Figure 3, with the exception of cases where acetone was used as the solvent, the average fiber diameter

(15) Bognitzi, M.; Czado, W.; Frese, T.; Schaper, A.; Hellwig, M.; Steinhart, M.; Greiner, A.; Wendorff, J. H. *Adv. Mater.* **2001**, *13*, 70.

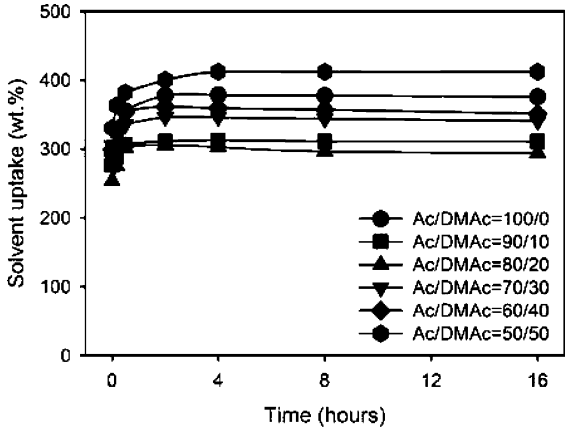

Figure 4. Electrolyte solution uptake behavior of the electrospun PVdF membranes in various polymer solutions.

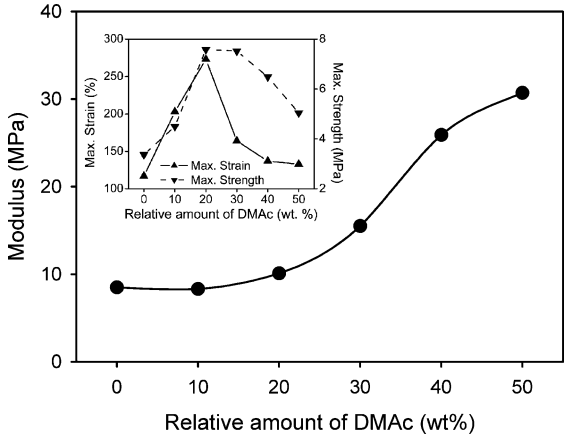

Figure 5. Mechanical properties of electrospun PVdF membranes prepared from polymer solutions of different composition.

and mean pore size of the electrospun PVdF membranes decreased with increasing DMAc content in the mixed-solvent system. When the content of DMAc was increased, the resulting fibers were noticeably thinner and had much smoother surfaces. It is expected that the less-volatile DMAc will hinder the rapid evaporation of the more-volatile acetone from the polymer solution during electrospinning. Consistent with this, elongation of the electrospun fibers was largely enhanced and the fibers had smooth surfaces when a high content of DMAc was present in the solvent. The average fiber diameter of the electrospun PVdF membranes prepared in acetone/DMAc (5/5, wt/wt) was found to be half that of the electrospun PVdF membranes prepared in acetone/DMAc (8/2, wt/wt). This indicates that the fiber diameter, surface morphology, and mean pore size strongly depend on the composition of the mixed solvent used in the electrospinning process.

The electrolyte solution uptake properties of electrospun PVdF membranes prepared using various mixed solvents are shown in Figure 4. The electrolyte solution uptake of electrospun PVdF membranes rapidly increased with soaking time in the early stages, but then ultimately slowed before reaching an equilibrium state. The electrospun PVdF membranes had unique pore structures that were formed by the interstices between ultrathin fibers and were fully interconnected. This membrane is capable of absorbing electrolyte solution in only a few hours, such that its uptake rate is faster than that of the porous membranes obtained by the phase-inversion technique. In our case, the uptake ability of electrospun PVdF membranes was found to depend largely on the physical properties of the fibers (see Table 2). The decrease in the average fiber diameter leads to an increase in electrolyte solution uptake due to the decrease in pore size and increase in specific surface area. It is generally known that membranes with small pores and high specific surface area have a great ability to absorb electrolyte solution. Contrary to this, however, electrospun PVdF membranes prepared using acetone and/or acetone/DMAc (9/1, wt/wt) consisted mainly of thick fibers but showed a large electrolyte solution uptake. This indicates that the electrolyte solution uptake depends on the surface morphology of the electrospun fibers as well as on the average fiber diameter. As shown in SEM images a and b in Figure 1, the electrospun PVdF membranes prepared using acetone contain pores, whereas those prepared using acetone/DMAc (9/1) have raised areas and wrinkles on their surfaces, indicating that they have higher specific surface area and higher electrolyte solution uptake than those with smooth surfaces. From these results, it is suggested that the electrolyte solution uptake ability largely depends on the average diameter and surface morphology of the fibers.

The mechanical properties of the electrospun membranes, including maximum strain, maximum strength, and modulus, are shown in Figure 5. The electrospun PVdF membranes prepared using acetone/DMAc (80/20, wt/wt) had the highest values of maximum strain and maximum strength. However, the modulus, which is an index of mechanical strength, increased with DMAc content in the polymer solution, with the electrospun PVdF membranes prepared in acetone/DMAc (50/50, wt/wt) showing the highest modulus. When electrospun PVdF membranes consist of small-diameter fibers, the physical cross-linking points between the fibers become more enhanced. It seems that physical cross-linking is one of the most important factors affecting the mechanical properties of the electrospun membranes. The solidity of the physical cross-linking depends on the solvent evaporation behavior during the electrospinning process. Polymer solutions containing a high concentration of acetone produce fibers that are easily solidified because of the rapid evaporation of the solvent during the flight toward the collector. Hence, the

Table 2. Physical and Mechanical Properties of Electrospun PVdF Fiber-Based Membranes

	sample					
	ESM-1	ESM-2	ESM-3	ESM-4	ESM-5	ESM-6
average fiber diameter (μm)	1.58	1.63	1.52	1.34	0.80	0.75
mean pore size (μm)	3.93	4.84	4.42	3.51	3.21	1.87
max. strain (%)	117	203	273	164	137	133
max. strength (MPa)	3.37	4.50	7.58	7.52	6.49	5.04
modulus (MPa)	8.46	8.29	9.84	15.5	25.6	29.7

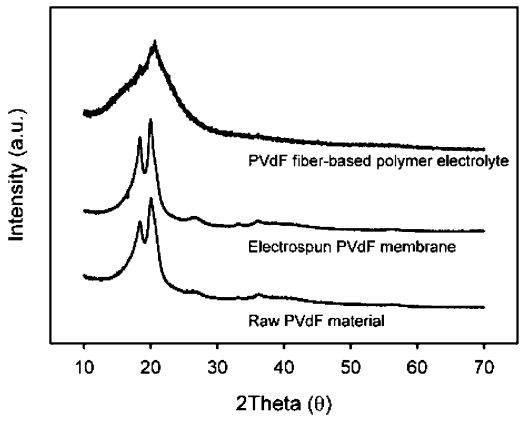

Figure 6. XRD spectra for the raw PVdF material, and the corresponding electrospun PVdF membrane and PVdF fiber-based polymer electrolyte.

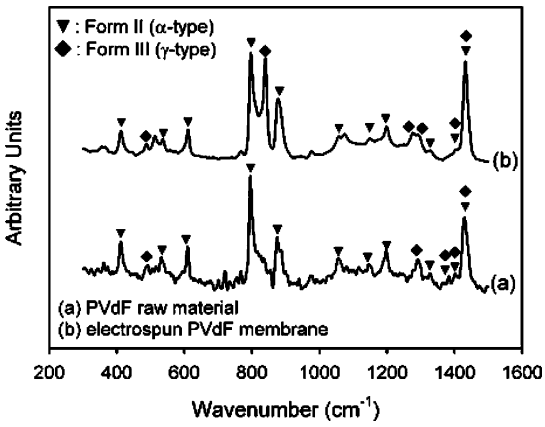

Figure 7. FT-Raman spectra for the raw PVdF material, and the corresponding electrospun PVdF membrane.

resulting PVdF membrane has relatively few physical cross-linking points between the fibers and thus forms a rather loose structure. However, an electrospun PVdF membrane prepared in a high concentration of DMAc has a relatively large number of physical cross-linking points with high solidity. Also, some DMAc will remain after electrospinning and will partially dissolve the surface of the PVdF fiber so that the physical cross-linking points may be significantly enhanced. Due to these factors, the electrospun PVdF membrane prepared using a high concentration of DMAc has superior mechanical properties.

From the present results, it is clear that electrospun PVdF membranes prepared using a mixed solvent of acetone/DMAc (5/5, wt/wt) are suitable as porous polymer membranes for use as polymer electrolytes, because they have the most appropriate physical properties, namely the thinnest average fiber diameter, the smallest pore size, a high solvent uptake, and sufficient mechanical strength. It is expected that this type of polymer electrolyte will have good electrochemical properties and maintain its framework in spite of the swelling induced by the electrolyte solution or the degradation brought about by the electrochemical reactions.

3.3. XRD Patterns of the Electrospun PVdF Membranes and Their Polymer Electrolytes. Figure 6 shows the X-ray diffraction (XRD) patterns of the PVdF raw material, the electrospun PVdF membrane, and the resulting polymer electrolyte in 1 M $LiPF_6$−EC/DMC/DEC (1/1/1). It is well-known that PVdF adopts one of the following three crystalline structures, depending on the preparation conditions: Form I (β-type crystal with planar zigzag conformation, orthorhombic), Form II (α-type crystal with TGTḠ, monoclinic), and Form III (γ-type crystal with TTTGTTTḠ, Monoclinic).[16,17] The PVdF raw material and the electrospun PVdF membrane have similar crystal structures, including two major peaks around 18 and 21°, and three minor peaks around 27, 36, and 57°. Most of the peaks are observed for all three crystalline forms of PVdF, whereas the peak at 27° is observed only for PVdF of Form II (α-type). It is estimated that the electrospun PVdF membrane contains Form II (α-type) with a monoclinic (pseudo-orthorhombic) structure. In addition, it is also possible to obtain another crystal structure comprising both Form I and Form III, because the three PVdF crystals have similar XRD spectra.

The XRD spectra of the corresponding polymer electrolytes showed broader peaks than the membrane itself. With the addition of liquid electrolyte to the membrane, the crystal structure of PVDF may be partially collapsed. In the case of the polymer electrolytes, the crystallinity of the PVdF decreased slightly, although the intensities of the peaks at 18.4 and 21.0° were markedly reduced, with the crystalline part of the PVdF still being observed in the XRD patterns. The minor peaks exhibited by the membrane were no longer detected in the XRD patterns of the polymer electrolytes. On the other hand, the broad peak around 21° overlapped the peaks of the original PVdF, and corresponded to the amorphous part of the PVdF.[16] When electrolyte solution was added to the electrospun PVdF membrane, the crystallinity of the PVdF phase was found to diminish slightly due to swelling. These results thus confirm that the electrolyte solution penetrates into the crystalline part of the PVdF and impedes the crystallization of the PVdF. However, the polymer electrolytes have sufficient mechanical strength because of the remaining crystalline phase in the electrospun PVdF membrane.

3.4. FT-Raman Spectra. *Comparison between the Raw PVdF Material and the Electrospun PVdF Membrane.* Vibrational spectroscopy is one of the most useful methods for confirming the crystal structure of the PVdF phase.[18,1919] FT-Raman spectra of the PVdF raw material and the resulting electrospun membrane are shown in Figure 7. From the XRD data, the crystal structure of the electrospun PVdF membrane was confirmed as Form II (α-type). In the FT-Raman spectrum, most of the bands corresponded to the Form II (α-type), whereas others were not assignable to this crystal structure. In particular, the weak bands at 490 and 1273 cm^{-1} corresponded to Form I and Form III, whereas the band at 839 cm^{-1} corresponded to Form III.[20−22] On the basis of these

(16) Tazaki, M.; Wada, R.; Okabe, M.; Homma, T. *J. Appl. Polym. Sci.* **1997**, *65*, 1517.
(17) Hasegawa, R.; Takahashi, Y.; Chatani, Y.; Tadokoro, H. *Polym. J.* **1972**, *3*, 600.
(18) Rodríguez-Cabello, J. C.; Merino, J. C.; Pastor, J. M. *Macromol. Chem. Phys.* **1995**, *196*, 815.
(19) Kobayashi, M.; Tashiro, K.; Tadokoro, H. *Macromolecules* **1975**, *8*, 158.
(20) Boccaccio, T.; Bottino, A.; Capannelli, G.; Piaggio, P. *J. Membr. Sci.* **2002**, *210*, 315.

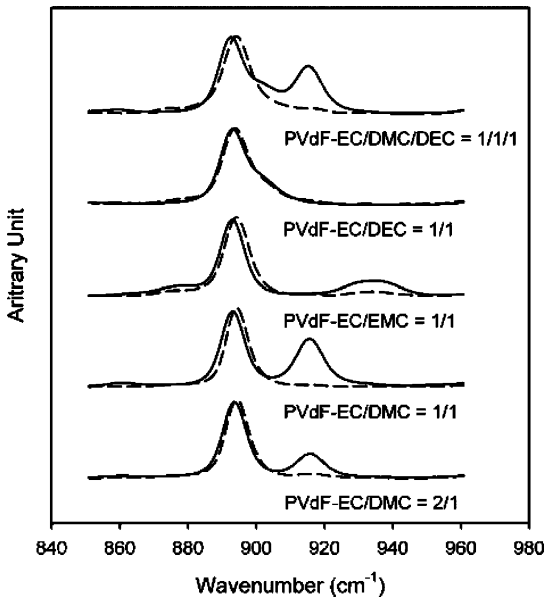

Figure 8. Normalized FT-Raman spectra of the EC symmetric ring breathing mode and C−O stretching mode of linear carbonates in mixed solvents (—) and polymer + mixed solvents (---).

findings, it is suggested that the electrospun PVdF membrane is a mixed-crystal structure comprising both Form II (α-type) and Form III (γ-type), with Form III (γ-type) possibly being enhanced during either the preparation of the polymer solution or electrospinning.

Comparison between Mixed-Solvent and Polymer−Mixed Solvent Systems. To investigate the interaction between the PVdF chain and the solvent molecules, we measured the FT-Raman spectra of mixed-solvent and polymer−mixed solvent systems. Figure 8 shows the FT-Raman spectra of the EC symmetric ring breathing mode and the C−O stretching mode of a linear alkyl carbonate in either a mixed-solvent or polymer−mixed solvent system. Previous work on the PVdF−solvent interaction in PVdF-based polymer electrolytes indicated that there is a specific interaction between the hydrogen in the methylene group of the PVdF polymer and the oxygen in the carbonyl group of the carbonate.[23−25]

In the FT-Raman spectra reported here, the PVdF chain interacted with the linear alkyl carbonate such that the C−O stretching mode of the linear alkyl carbonate was suppressed, as shown for the PVdF−mixed solvent system. However, the FT-Raman spectrum of the PVdF−EC/DEC (1/1) system was similar to that of the mixed solvent with EC/DEC (1/1). It is therefore assumed that the DEC molecule interacts weakly with PVdF. It is well-known that the interaction between the polymer and the solvent takes place in the crystalline regions of the host polymer;[26] hence these interactions will affect the crystallinity of the host polymer. However, DEC has a larger molecular size than either DMC or EMC, making it difficult for DEC to penetrate into the crystalline region of PVdF. On the other hand, the vibrational bands for the ring breathing mode of EC were not suppressed, but showed a slight shift in the high frequency. This shift is consistent with a weak interaction between the hydrogen in the methylene group of PVdF and the oxygen in the carbonyl group of the EC molecule.

From these results, it is clear that with the exception of DEC, interactions between the PVdF chain and the linear alkyl carbonate molecules are commonplace. In addition, a weak interaction between the PVdF chain and EC molecule was inferred from the FT-Raman spectra of the polymer−mixed solvent systems. The interaction between the PVdF chain and the carbonate molecule largely depends on the molecular weight and conformation of the carbonate molecules.

Comparison between Electrolyte Solutions and Their Polymer Electrolytes. Figure 9 shows the FT-Raman spectra of the ring breathing mode of EC and the C−O stretching mode of the linear alkyl carbonate in the electrolyte solutions and the resulting electrospun PVdF fiber-based polymer electrolytes. In these cases, the C−O stretching modes of the linear alkyl carbonates were also suppressed. Thus, all other bands resulting from interactions between the polymer and the linear alkyl carbonate molecules were not observed. Although the linear alkyl carbonate molecules in the electrolyte solution are able to interact with either the lithium ions or the PVdF chain, the C═O group of the linear alkyl carbonate molecules show a strong preference for the methylene groups of the PVdF chain. The C−O stretching modes of the linear alkyl carbonate molecules are thought to be "frozen" by this interaction, causing their bands to be suppressed. However, the FT-Raman spectrum of the PVdF-fiber based polymer electrolyte in 1 M $LiPF_6$−EC/DEC (1/1) was similar to that of the native electrolyte solution. A similar result was also observed in the PVdF−EC/DEC (1/1) system (Figure 7). This implies that the PVdF chain rarely interacts with the DEC molecules. On the other hand, the symmetric ring breathing mode of the EC molecule was much less affected than the C−O stretching mode of the linear alkyl carbonate molecules. Here, this band was only slightly shifted toward higher frequencies, as shown in Figure 8. Unlike the aliphatic carbonate with an open molecular chain structure, the cyclic ring strain in the EC molecule may resist changes in the symmetric ring breathing mode as a result of these interactions between the C═O group and the methylene group of PVdF.

These results confirm that linear alkyl carbonate molecules primarily interact with polymer chains, reducing the crystallinity of the polymer matrix by penetrating into the crystal phase and interacting with the methylene group of the PVdF chain, thereby assisting in the transport of lithium ions solvated by the EC molecules. Although linear alkyl carbonate molecules are thought to be only partially involved in the solvation of lithium salts and Li^+ ion conduction, our results indicate that EC molecules are highly involved in the solvation of the lithium salt and interaction with Li^+ ions. Hence, lithium ion conduction may depend on the solvation of the Li^+ ions by EC molecules.

3.5. Electrochemical Properties of Polymer Electrolytes with Electrospun PVdF Membranes. *Ionic Conductivities*.

(21) Lu, F. J.; Hsu, S. L. *Polymer* **1984**, *25*, 1247.
(22) Matsushige, K.; Takemura, T. *J. Cryst. Growth* **1980**, *48*, 343.
(23) Song, J. M.; Kang, H. R.; Kim, S. W.; Lee, W. M.; Kim, H. T. *Electrochim. Acta* **2003**, *48*, 1339.
(24) Chen, N.; Hong, L. *Polymer* **2002**, *43*, 1429.
(25) Jacob, M. M. A.; Arof, A. K. *Electrochim. Acta* **2000**, *45*, 1701.
(26) Chintapalli, S.; Frech, R. *Solid State Ionics* **1996**, *86−88*, 341.

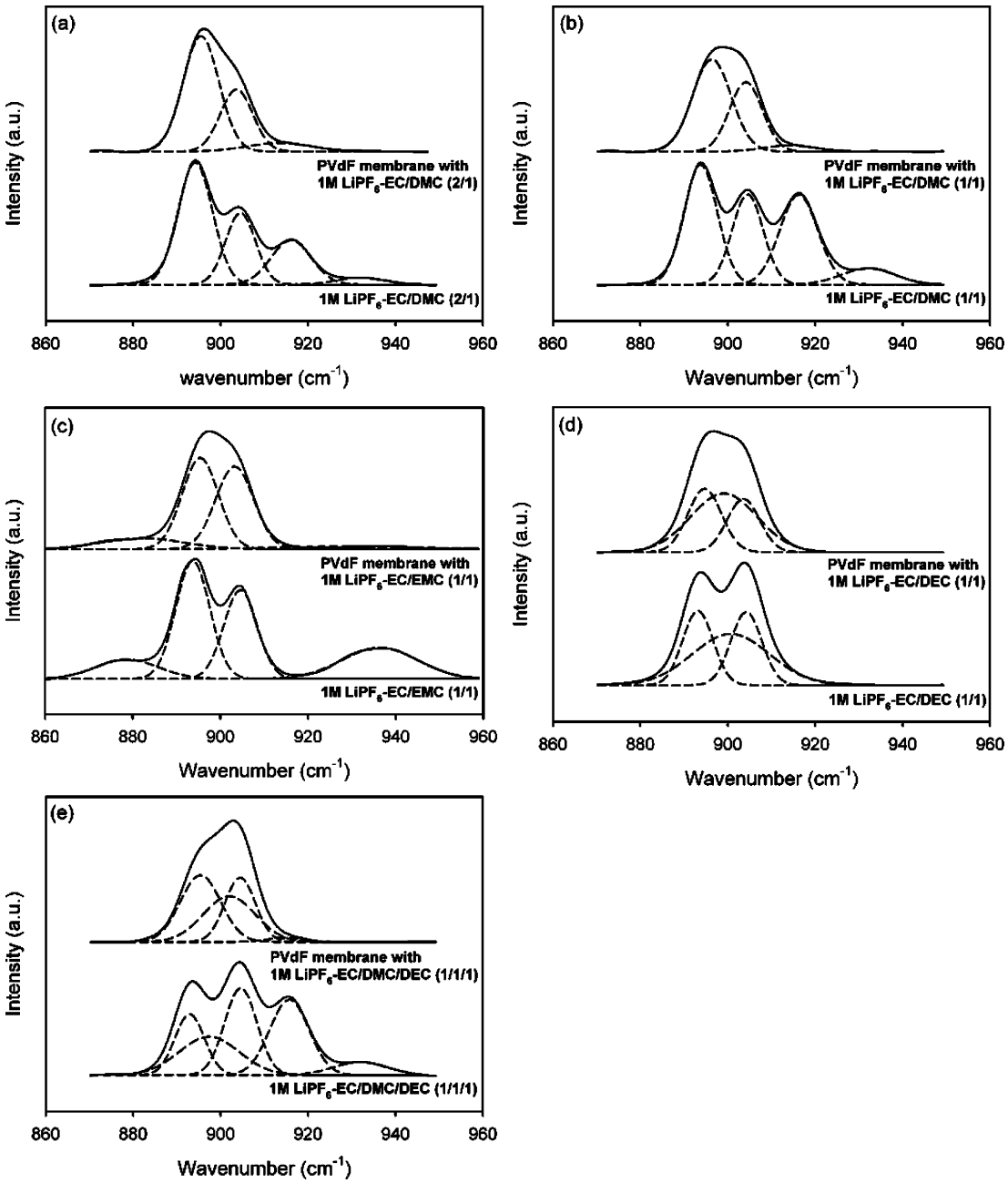

Figure 9. Normalized FT-Raman spectra of the EC symmetric ring breathing mode and C−O stretching mode of linear carbonates in electrolyte solutions and PVdF fiber-based polymer electrolytes.

The ionic conductivities of PVdF fiber-based polymer electrolytes are shown in Figure 10. Previously, we demonstrated that electrospun PVdF nanofibrous polymer electrolytes show high ionic conductivity at room temperature.[13] Although all electrospun PVdF fiber-based polymer electrolytes are composed of PVdF microfibers with high crystallinity, they also show high ionic conductivities above 1.0×10^{-3} S/cm at room temperature. From the FT-Raman data, we confirmed that the major conduction pathway resulted from Li^+-solvated EC molecules moving through the interconnected pores of the electrospun PVdF fiber-based membrane. As such, the ion conduction behavior was largely dependent on the physicochemical properties of the electrolyte solution. Hence, ionic conductivities may be enhanced by the swollen portions of the PVdF via interaction between the PVdF chains and the linear alkyl carbonates.

The conduction behavior of PVdF fiber-based polymer electrolytes in the low-temperature region of −20 to 10 °C largely depends on the freezing properties of the carbonate solvents in the electrolyte solution. It is well-known that the melting points of carbonate solvents decrease in the order of EC (36.4 °C) > DMC (4.6 °C) > EMC (−53.0 °C) > DEC (−74.3 °C). In the systems considered here, the ionic conductivity decreased with increasing EC content, because the crystalline part of the EC molecules hindered lithium-ion transport. Specifically, the electrospun PVdF fiber-based polymer electrolyte with 1 M $LiPF_6$−EC/DMC/DEC (1/1/1) showed the highest ionic conductivity, whereas that with 1 M $LiPF_6$−EC/DMC (2/1) showed the lowest ionic conductivity. On the other hand, the solidification temperature of the mixed-solvent system (with the same weight fraction of EC) is expected to decrease in the order EC/DMC > EC/

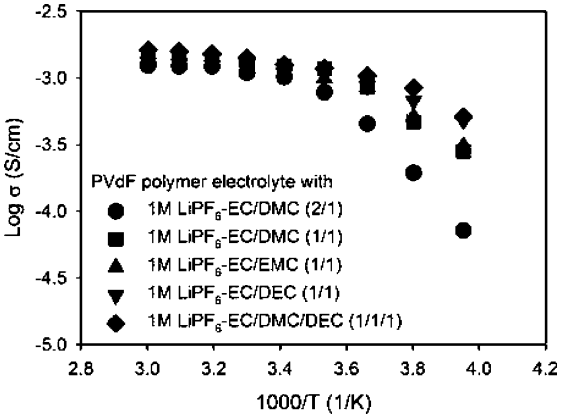

Figure 10. Ionic conductivities of electrospun PVdF-based fibrous polymer electrolytes.

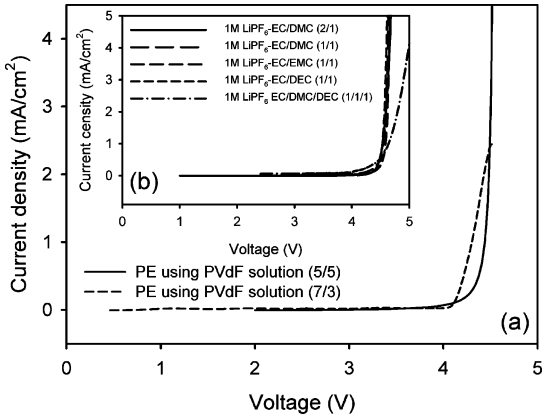

Figure 11. Electrochemical stability windows of electrospun PVdF fiber-based polymer electrolytes.

EMC > EC/DEC, because the linear alkyl carbonate molecules suppress the solidification of EC. Hence, the observed ionic conductivities were found to decrease in the order EC/DEC > EC/EMC > EC/DMC among the electrospun PVdF fiber-based polymer electrolytes with the same weight fraction of EC.

In the high-temperature region between 20 and 60 °C, the electrolyte solution in the pores of the electrospun PVdF fiber-based membranes was completely liquid. In this temperature range, the electrospun PVdF fiber-based polymer electrolytes showed high ionic conductivities of up to 1.0×10^{-3} S/cm, whereas their ionic conductivities decreased in the order of 1 M $LiPF_6$−EC/DMC/DEC (1/1/1) > 1 M $LiPF_6$−EC/DMC (1/1) > 1 M $LiPF_6$−EC/EMC (1/1) > 1 M $LiPF_6$−EC/DEC (1/1) > 1 M $LiPF_6$−EC/DMC (2/1). Moreover, the ionic conductivities depended on the mobility of the electrolyte solution in the pores of the electrospun PVdF fiber-based membrane. It is noted that the mobility of the electrolyte solution is directly related to its viscosity, where the viscosities of the solvents decrease in the order EC (1.93 cP) > DEC (0.753 cP) > EMC (0.648 cP) > DMC (0.589 cP). Therefore, the electrospun PVdF fiber-based polymer electrolyte with 1 M $LiPF_6$−EC/DMC (2/1) has the highest EC content and showed the lowest ionic conductivity because of its higher viscosity. On the other hand, the polymer electrolyte with 1 M $LiPF_6$−EC/DMC/DEC (1/1/1) has the lowest EC content and showed the highest ionic conductivity. Thus, it is expected that the viscosities of the electrolyte solutions with the same weight fraction of EC will decrease in the order EC/DEC > EC/EMC > EC/DMC. The ionic conductivities of the electrospun PVdF fiber-based polymer electrolytes show the same trend as the viscosities of the electrolyte solutions, because the electrolyte solutions fill the pores of the electrospun PVdF fiber-based membrane through weak interactions with the polymer chain.

These results indicate that the electrospun PVdF fiber-based polymer electrolytes show sufficient ionic conductivity for use in lithium cells. In addition, they confirm that the ionic conductivities of the electrospun PVdF fiber-based polymer electrolytes depend mainly on the physicochemical properties of the electrolyte solution within the pores and only slightly on the interaction between the polymer chain and the solvent molecules.

Electrochemical Stability Windows. The electrochemical stability windows of the PVdF-based polymer electrolytes containing various electrolyte solutions are shown in Figure 11. Although the electrospun PVdF fiber-based membranes have large pores and high porosity, the polymer electrolytes prepared using electrospun PVdF membranes show oxidation stabilities up to 4.5 V. The electrospun PVdF fiber-based polymer electrolyte prepared from 17 wt % PVdF−acetone/DMAc (5/5) had a larger electrochemical stability window than that prepared from 17 wt % PVdF−acetone/DMAc (7/3). Because the electrospun PVdF membrane prepared from 17 wt % PVdF−acetone/DMAc (5/5) has a narrower fiber diameter and a smaller pore size than that prepared from 17 wt % PVdF−acetone/DMAc (7/3), the electrolyte solution is more tightly trapped in the pores of the former membrane. Thus, the interaction between the PVdF chain and the linear alkyl carbonate in the electrospun PVdF fiber-based polymer electrolyte can be confirmed from the FT-Raman data. Hence, this interaction will contribute to the enhancement of the electrochemical stability window.

From these results, it can be seen that the electrospun PVdF fiber-based polymer electrolytes show adequate electrochemical stability windows for use in lithium cells. In addition, the electrochemical stability window depends on the pore size of the electrospun membrane and is therefore enhanced by interactions between the PVdF chain and the linear alkyl carbonate molecules.

3.6. Charge−Discharge Performance of PrototypeCells with Electrospun PVdF Membranes. *Cycle Performance at a Charge/Discharge Rate of 0.5C/0.5C*. The following MCMB/electrospun PVdF fiber-based polymer electrolyte/$LiCoO_2$ prototype cells were constructed in order to demonstrate the use of the electrospun PVdF membranes in lithium cells. Figure 12a shows the discharge capacities for a graphite/PVdF-based polymer electrolyte/$LiCoO_2$ cell at a charge/discharge rate of 0.5C/0.5C. The prototype cells showed different cyclic performances depending on the composition of the electrolyte solution. Smart and co-workers reported that the relative ability of solvents to form ionically conductive and protecting surface films on electrodes, especially the anode, decreased in the order of EC > DMC > EMC > DEC, whereas a reverse trend is observed for the melting points of the solvents and their respective viscosities.[27] Thus, it is known that electrolyte solvent

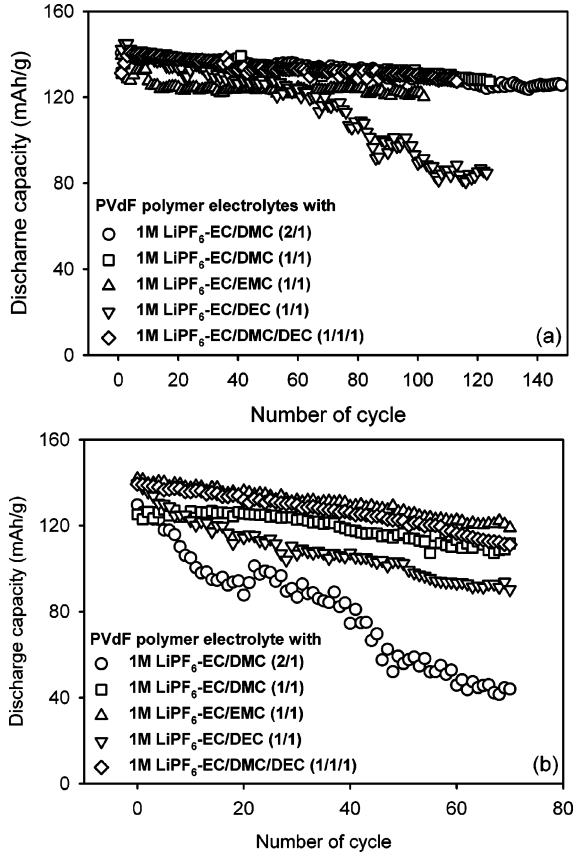

Figure 12. Cycle performances of lithium cells with PVdF fiber-based polymer electrolytes at charge/discharge rates of (a) 0.5C/0.5C and (b) 1.0C/1.0C.

molecules co-intercalate with the Li^+ ions in the graphite layers during charging.[28,29] It has been suggested that such solvent co-intercalation takes place more extensively in the EC/DEC system than in the EC/DMC system, because the DEC molecules are known to enhance co-intercalation of the solvent.[30] These co-intercalated solvent molecules were not easily released from the graphite electrode and deformed the inactive materials that formed unstable passivation layers during cycling performance. Therefore, the irreversible capacities of the EC/DEC system in the first and second cycles were larger than those of other systems, because the EC/DEC system shows a more inhomogeneous passivation layer than the EC/DMC system.

The prototype cell with 1 M $LiPF_6$−EC/DMC/DEC (1/1/1) showed the highest discharge capacity (about 97% of the initial discharge capacity after 113 cycles) and the most stable cyclic performance. Although this cell contained DEC molecules, its cycle performance was only slightly affected by DEC. In the polymer−mixed solvent with EC/DMC/DEC (1/1/1), we confirmed that most of the DEC molecules interacted with the PVdF polymer chain and were trapped in the pores of the electrospun PVdF membrane. Therefore, the C−O stretching mode of DEC was suppressed, as shown in Figure 7. From this point of view, the electrospun PVdF fiber-based polymer electrolyte with 1 M $LiPF_6$−EC/DMC/DEC (1/1/1) may show the same behavior. The prototype cell of this system had few free DEC molecules available to decompose easily during cycling and showed a high discharge capacity and stable cycling.

Similarly, the lack of free DEC molecules in the prototype cells produced using 1 M $LiPF_6$−EC/DMC solution also had a high discharge capacity and stable cyclic performance. The prototype cell with 1 M $LiPF_6$−EC/DMC (2/1) had a lower discharge capacity than that with 1 M $LiPF_6$-EC/DMC (1/1), which is typical behavior of cells with a high EC content. If the polymer electrolyte has a high EC content, then it usually has a relatively low ionic conductivity and slow ion mobility due to the high viscosity and crystallizing properties of EC in the low-temperature region. Hence, the discharge capacity of the prototype cell with 1 M $LiPF_6$−EC/DMC (2/1) was lower than that of the cell with 1 M $LiPF_6$−EC/DMC (1/1).

The prototype cell with 1 M $LiPF_6$−EC/DEC (1/1) had the highest initial discharge capacity, but exhibited rapid capacity fading behavior. This prototype cell had only 59.5% of the initial discharge capacity at a charge/discharge rate of 0.5C/0.5C after 123 cycles. These results suggest that the large amount of free DEC molecules participate in co-intercalation with Li^+ ions and are not easily released from the graphite electrode.

From the FT-Raman results, it is confirmed that DMC molecules combine tightly with the polymer chains, whereas DEC molecules move freely through the three-dimensionally interconnected pores. As such, DEC molecules may be more easily decomposed by electrochemical reaction to form an unstable passivation layer during cycling, resulting in a drastic decrease in the capacity of the prototype cell containing 1 M $LiPF_6$−EC/DEC (1/1). Finally, lithium cells with a high DEC content are not good for long-term cycling, whereas those with DMC or EMC show good cycle performance, because DMC or EMC may be decomposed less and are not easily inserted into the graphite anode because of their better binding properties with polymer chains.

Cycle Performance at a Charge/Discharge Rate of 1.0C/1.0C. The cycle performances of prototype cells at a charge/discharge rate of 1.0C/1.0C are shown in Figure 12b. The discharge capacities of these prototype cells rapidly decreased and showed quite different behavior compared with those at the charge/discharge rate of 0.5C/0.5C. Although the prototype cell with 1 M $LiPF_6$−EC/DMC (2/1) showed a stable cycle performance and a high discharge capacity at a charge/discharge rate of 0.5C/0.5C, this cell under the 1.0C/1.0C rate showed the worst cycle performance and retained only 32.1% of the initial discharge capacity after 80 cycles. This poor performance is due to the electrospun PVdF fiber-based polymer electrolyte with 1 M $LiPF_6$−EC/DMC (2/1) having the lowest ionic conductivity. The prototype cell with the polymer electrolyte having a high EC content showed poor cycle performance at high C-rates. During charging and discharging, lithium ions moved slowly between the two

(27) Smart, M. C.; Ratnakumar, B. V.; Whitcanack, L. D.; Chin, K. B.; Surampudi, S.; Croft, H.; Tice, D.; Staniewicz, R. *J. Power Sources* **2003**, *119*−*121*, 349.
(28) Jeong, S. K.; Inaba, M.; Iriyama, Y.; Abe, T.; Ogumi, Z. *Electrochim. Acta* **2002**, *47*, 1975.
(29) Yang, C. R.; Song, J. Y.; Wang, Y. Y.; Wan, C. C. *J. Appl. Electrochem.* **2000**, *30*, 29.
(30) Zhuang, G.; Chen, Y.; Ross, Jr. P. N. J. *Langmuir* **1999**, *15*, 1470.

electrodes. The prototype cell with 1 M $LiPF_6$−EC/DEC (1/1) also showed a declining capacity with an initial discharge capacity of 64.7% after 80 cycles. It is estimated that the cycle performance of the polymer electrolyte cell with 1 M $LiPF_6$−EC/DEC (1/1) is affected in two ways: (1) a lowering of the ionic conductivity, and (2) the occurrence of an intense intercalation of DEC molecules during charging.

Although the prototype cell with 1 M $LiPF_6$−EC/DMC/DEC (1/1/1) contained DEC, it showed a stable cycle performance and had a high discharge capacity of 79.8% after 80 cycles. From the FT-Raman data, it is confirmed that most of the DEC molecules interacted with the PVdF chains, suppressing the vibrational mode, but did not easily intercalate during charging. This cell had the highest ionic conductivity because it had the lowest EC content. On the other hand, the prototype cells with 1 M $LiPF_6$−EC/DMC (1/1) and with 1 M $LiPF_6$−EC/EMC, which did not contain DEC molecules, were more easily able to intercalate between graphite layers during charging. Consequently, these prototype cells showed stable cycle performances and high discharge capacities.

These results show that the cycling performances of prototype cells at charge/discharge rates of 1.0/1.0C strongly depend on the ionic conductivity and DEC content in the polymer electrolyte.

3.7. Electrospun PVdF Membranes after Cycle Life Testing. To investigate the microscopic changes in the electrospun PVdF fiber-based membranes after cycling, we carried out SEM and X-ray diffraction measurements. Images a and b of Figure 13 show SEM images of the electrospun PVdF membranes before and after washing in 2-propanol to remove the remaining electrolyte solution. The average fiber diameter after cycling was 0.77 μm, which was almost the same as that before cycling (0.75 μm). In addition, there were no significant changes in the surface morphology compared with the as-prepared electrospun PVdF fiber-based membranes.

On the other hand, the electrospun PVdF-based polymer electrolyte formed after cycling had quite a broad XRD spectrum, but still contained the crystal phase of PVdF, as shown in Figure 13c. Although the major peak for the PVdF crystal phase was rarely distinguished because of overlap with the gel phase peak, small peaks for the PVdF crystal phase were still observed in the range between 30 and 50°.

These results show that the fiber diameters of the electrospun PVdF fiber-based membranes were slightly changed by swelling during cycling and were rarely affected by the charging and discharging. The PVdF fiber-based framework was maintained in spite of swelling resulting from the penetration of the electrolyte solution into the fibers and by electrochemical cycling. PVdF has a low affinity for electrolyte solutions and thus represents an attractive material for use as the matrix in polymer electrolytes with excellent electrochemical properties and adequate mechanical properties.

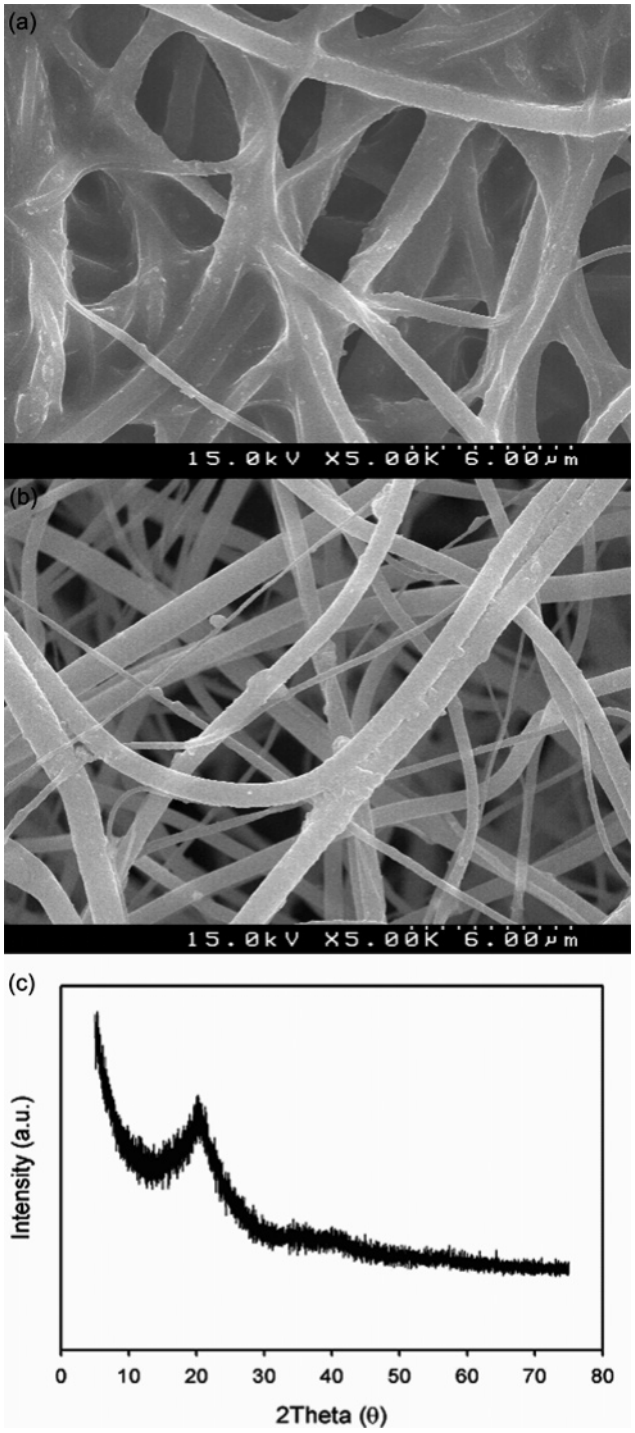

Figure 13. SEM image and XRD spectrum for the PVdF fiber-based polymer electrolytes with 1 M $LiPF_6$-EC/DMC/DEC (1/1/1) after cycle performance.

4. Conclusions

Porous PVdF fiber-based membranes were prepared using the electrospinning technique. According to the composition of the polymer solution, the PVdF fibers of the electrospun membranes had quite different physical properties, including surface morphology, solvent uptake ability, average fiber diameter, and mechanical strength. Electrospun PVdF fiber-based polymer electrolytes were prepared by immersion of the electrospun membrane in electrolyte solutions. FT-Raman spectroscopic data showed that the lithium ions predominately associated with the EC molecules, indicating that Li^+-solvated EC is a major mobile ionic species in these polymer electrolytes. In addition, the PVdF chain showed good interaction with all but one of the linear alkyl carbonate

molecules studied, namely diethyl carbonate. This interaction influences the swelling of PVdF to form a gel phase and is responsible for enhancement of the electrochemical properties.

The PVdF fiber-based polymer electrolytes showed good electrochemical properties, including high ionic conductivity and wide electrochemical stability windows. The ionic conductivities of these PVdF fiber-based polymer electrolytes were above 1.0×10^{-3} S/cm at room temperature and were dependent on the physicochemical properties of the electrolyte solution, including viscosity and freezing point. In addition, the interaction between the PVdF chains and the linear alkyl carbonates enhances the electrochemical properties of the electrospun PVdF fiber-based polymer electrolytes.

Most of the prototype cells showed a high discharge capacity and stable cycling performance, whereas those with high contents of EC and/or DEC showed poor cycling performance, especially at high C-rates. Therefore, the cycling performances of the prototype cells strongly depend on the interactions between the molecules in the PVdF fiber-based polymer electrolytes.

The present experiments further confirmed that the PVdF fiber-based framework is preserved after cycling. Thus, the electrospun PVdF fiber-based membranes have excellent electrochemical and adequate mechanical properties and are a good polymer matrix for use in lithium/polymer cells.

Acknowledgment. We gratefully acknowledge the Nanofiber R&D Center of the Samshin Creation Co. (Korea) for their assistance in this research.

Supporting Information Available: Additional SEM images. This material is available free of charge via the Internet at http://pubs.acs.org.

CM060223+